MOLE-BERT: RETHINKING PRE-TRAINING GRAPH NEURAL NETWORKS FOR MOLECULES

Anonymous authors
Paper under double-blind review

ABSTRACT

Recent years have witnessed the prosperity of pre-training graph neural networks (GNNs) for molecules. Typically, following the Masked Language Modeling (MLM) task of BERT (Devlin et al., 2019), Hu et al. (2020) first randomly mask the atom types and then pre-train the GNNs to predict them. However, unlike MLM, this pre-training task named AttrMask is too simple to learn informative molecular representations due to the extremely small and unbalanced atom 'vocabulary'. As a remedy, we adopt the encoder of a variant of VQ-VAE (Van Den Oord et al., 2017) as a context-aware tokenizer to encode atoms as meaningful discrete values, which can enlarge the atom vocabulary size and mitigate the quantitative divergence between dominant (e.g., carbons) and rare atoms (e.g., phosphorus). With the enlarged atom 'vocabulary', we propose a novel node-level pre-training task, dubbed Masked Atoms Modeling (**MAM**), to randomly mask the discrete values and pre-train GNNs to predict them. MAM mitigates the negative transfer issue of AttrMask and can be combined with various pre-training tasks to advance their performance. Furthermore, for graph-level pre-training, we propose triplet masked contrastive learning (**TMCL**) to model varying degrees of semantic similarity between molecules, which is especially effective for molecule retrieval. MAM and TMCL constitute a novel pre-training framework, **Mole-BERT**, which can match or outperform state-of-the-art methods that require expensive domain knowledge as guidance. The codes, the tokenizer, and the pre-trained models will be released.

1 INTRODUCTION

Pre-training Language Models (PLMs) have revolutionized the landscape of Natural Language Processing (NLP). The representative one is BERT (Devlin et al., 2019), whose Masked Language Modeling (MLM) pre-training task first randomly masks some proportions of tokens within a text, and then recovers the masked tokens based on the encoding results of the corrupted text. Although BERT also includes the pre-training task of next sentence prediction, MLM is verified as the only success recipe for BERT (Liu et al., 2019; Raffel et al., 2020). Inspired by this, MLM-style pre-training task has been extended to many other domains (Hu et al., 2020; Dosovitskiy et al., 2021; He et al., 2022).

Molecules can be represented naturally as graphs with their atoms as nodes and chemical bonds as edges. Hence, Graph Neural Networks (GNNs) can be utilized to process molecular graph data. To exploit the abundant unlabeled molecules, tremendous efforts have been devoted to pre-training GNNs for molecular graph representations (Xia et al., 2022b). The pioneering work (Hu et al., 2020) on this topic first pre-trains GNNs with a MLM-style pre-training task (AttrMask) on large-scale unlabeled molecular graph datasets. Specifically, they randomly mask some proportions of atoms and then pre-train the models to predict them. AttrMask has emerged as a fundamental pre-training task and many subsequent works adopt it as a sub-task for pre-training (Zhang et al., 2021; Li et al., 2021a). During the tuning stage, researchers replace the top layer of the pre-trained models with a task-specific sub-network and train the new model with the labeled molecules of the downstream tasks. However, Hu et al. (2020) observe that pre-training only with AttrMask (node-level pre-training task) will incur the negative transfer issue (i.e., pre-trained models fall behind no pre-trained models) sometimes. Intuitively, they think this phenomenon can be attributed to the lack of graph-level pre-training tasks and thus introduce supervised graph-level pre-training strategies, which are impractical because the labels are often expensive or unavailable. Additionally, some supervised pre-training tasks unrelated to the downstream task of interest can even degrade the downstream performance (Hu et al., 2020).

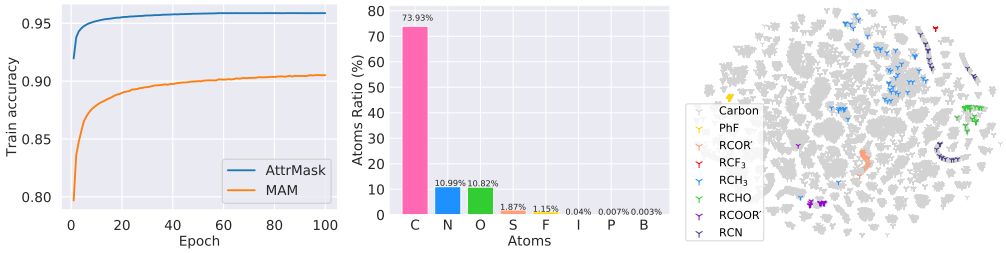

(a) (b) (c)

Figure 1: **(a)**: Pre-training accuracy curves of AttrMask and MAM; **(b)**: The atoms ratios of various chemical elements in the pre-training datasets; **(c)**: The t-SNE visualization of the carbon representations learned by the proposed tokenizer. Firstly, we randomly sample 30, 000 carbons from the QM9 dataset (Ruddigkeit et al., 2012). Among them, 250 are randomly chosen and colored based on the types of functional groups that carbons belong to. Both R and R' are the abbreviations for groups in the rest of a molecule. The details of the 7 local structure groups are listed in Appendix K.

In this paper, we provide a second voice on this predominant belief and aim to explain the negative transfer in molecular graph pre-training. Firstly, as can be observed in Figure 1(a), the pre-training accuracy of AttrMask converges to $\sim 96\%$ quickly, which indicates AttrMask task (118-way classification, 118 is the number of common chemical elements in nature) is extremely simple for the small atom vocabulary size. The atom vocabulary is the set of unique atom types of common chemical elements in nature. In contrast, the training accuracy of the MLM task ($\sim$ 30k-way classification) in BERT only grows to 70% and hardly converges for the large text vocabulary size ($\sim$ 30k tokens) (Kosec et al., 2021). Text vocabulary is the set of unique tokens in the corpus. Secondly, the quantitative divergence between different atoms is extremely significant (see Figure 1(b)), which will bias the models' prediction toward dominant atoms (e.g., carbons) and lead to fast convergence. Previous works (Clark et al., 2020; Robinson et al., 2021) have revealed that simple pre-training tasks will capture less transferable knowledge and impair the generalization or adaptation to novel tasks.

Tokenization is the first step in any NLP pipeline, which separates a piece of text into smaller units called tokens (Sennrich et al., 2015; Wu et al., 2016). Hence, pre-training language models include two stages: the first stage is tokenizer training and the second stage is language models pre-training. However, for GNNs pre-training, previous works adopt the atoms' types as tokens, which will result in a small-size and unbalanced atom vocabulary. We argue that atoms with different contexts should be tokenized into different discrete values even if they belong to the same type. For example, Aldehyde carbons and ester carbons indicate different properties of molecules even if both of them are carbons. Hence, we introduce a context-aware tokenizer to encode atoms to meaningful discrete values. Specifically, these discrete values are the latent codes of a variant of graph VQ-VAE (Van Den Oord et al., 2017). The tokenizer is context-aware because the encoder of graph VQ-VAE is a GNN model. In this way, we can categorize the dominant atoms (e.g., carbons) into several chemically meaningful sub-classes (e.g., aldehyde carbons, ester carbons, etc.) considering the atoms' context, which will enlarge the atom vocabulary size and mitigate the quantitative divergence between dominant and rare atoms. To support the above claims, we provide the t-SNE visualization of carbon representations learned by the proposed tokenizer in Figure 1(c). As can be observed, the representations of carbons are clustered based on types of functional groups, which indicates our tokenizer can encode atoms to chemically meaningful values. With the new vocabulary, we propose a node-level pre-training task, dubbed Masked Atoms Modeling (MAM), to randomly mask the discrete values and pre-train GNNs to predict them. Alternatively, we can also regress the output atoms embeddings of VQ-VAE as the pre-training objective, which we study in Appendix D. Additionally, we can also tokenize the chemical bonds to boost the performance, which we elaborate in Appendix F. For molecular graph-level pre-training, graph contrastive learning (You et al., 2020) is a feasible pre-training strategy. However, contrastive approaches push different molecules away equally regardless of their varying degrees of similarities. To remedy this deficiency, we propose triplet masked contrastive learning (TMCL), which mimics the varying degrees of molecular similarities with different masking ratios.

We highlight the following contributions: **(i)** We find the negative transfer issue of AttrMask can be attributed to the extremely small and unbalanced atom vocabulary. **(ii)** As a remedy, we contribute a

context-aware tokenizer for molecular graphs using a variant of VQ-VAE. Also, the tokenizer can be re-used as an off-the-shelf tool for subsequent works like the NLP community. **(iii)** With the new vocabulary, we propose a tailored pre-training task, MAM, to alleviate the negative transfer issue. MAM serves as a fundamental pre-training task and can be combined with various pre-training tasks to advance their performance. **(iv)** We propose a novel graph-level pre-training task, TMCL, to consider varying degrees of similarities between molecules, which is especially effective for molecule retrieval. **(v)** We combine MAM and TMCL as a joint pre-training framework (Mole-BERT), which matches or outperforms state-of-the-art models that require expensive domain knowledge as guidance.

2 Related Work

2.1 Pre-training GNNs for Molecules

Recent years have witnessed the proliferation of Graph Neural Networks (GNNs) in molecular representation learning. While effective and prevalent, they require expensive annotations and barely generalize to unseen molecules, which pose a hurdle to practical applications. To remedy these deficiencies, tremendous efforts have been devoted to pre-training molecular graphs. One line of these works follows the contrastive paradigm (Zhu et al., 2021b;a; Qiu et al., 2020; Thakoor et al., 2022). For molecular pre-training, GraphCL (You et al., 2020) and its variants (You et al., 2021; Suresh et al., 2021; Xia et al., 2022a; Wang et al., 2022; Sun et al., 2021; Fang et al., 2022b) embed augmented versions of the anchor molecular graph close to each other and push the embeddings of other molecules apart. Additionally, DGI (Velickovic et al., 2019) and InfoGraph (Sun et al., 2020a) is proposed to obtain expressive representations for graphs or nodes via maximizing the mutual information between graph-level representations and substructure-level representations of different granularity. The other line of work adopts generative or predictive pretext tasks. Typically, GPT-GNN (Hu & others., 2020) introduces an attributed graph generation task to pre-train GNNs so that they can capture the structural and semantic properties of the graph. For molecular graph pre-training, Hu et al. (2020) and Li et al. (2021b) conduct attribute and structure prediction at the level of individual nodes as well as entire graphs. To capture the rich information in molecular graph motifs, GROVER (Rong et al., 2020a) and MGSSL (Zhang et al., 2021) propose to predict or generate the motifs. Considering that 3D geometric information also plays a vital role in predicting molecular properties, several recent works (Liu et al., 2022a; Stärk et al., 2021; Fang et al., 2022a; Zhu et al., 2022) pre-train the GNN encoders on molecular datasets with 3D geometric information. We recommend readers refer to several recent reviews (Liu et al., 2022b; Xie et al., 2022) for more relevant literatures. Many above-mentioned works adopt AttrMask (Hu et al., 2020) as a fundamental pre-training sub-task. However, AttrMask will incur the negative transfer issue sometimes. We explain this phenomenon and contribute a novel pre-training strategy to remedy this deficiency.

2.2 MLM-style Pre-training Strategies

The masked language modeling (MLM) task proposed in BERT Devlin et al., 2019 has emerged as one of the most popular and successful pre-training tasks. Empirically, RoBERTa (Liu et al., 2019) finds that MLM is the only success recipe of BERT and discards the sentence-level task in BERT. Also, BART (Lewis et al., 2019) and T5 (Raffel et al., 2020) both observed that MLM is often the most effective task. Alternatively, various MLM variants improve MLM with dynamic masking strategy (Liu et al., 2019) and blockwise masking strategy (Joshi et al., 2020). Additionally, XLNet (Yang et al., 2019) proposes permutation language modeling that conducts MLM in an autoregressive manner. UniLM (Bao et al., 2020) uses pseudo MLM which unifies autoregressive and MLM tasks. Inspired by these advances, for vision transformer pre-training, the model receives incomplete images with a large portion of the patches removed and learns to reconstruct the missing contents on low-level image pixels (He et al., 2022; Li et al., 2021c; Dosovitskiy et al., 2021; Chen et al., 2020), high-level semantics (Bao et al., 2021) or hand-crafted feature descriptors (Wei et al., 2022). Different from the above-mentioned works, our MAM adopts the encoder of VQ-VAE as the atoms tokenizer, which discretizes a continuous semantic space to discrete codes in a context-aware manner. Moreover, we observe that atoms of different types might be allocated with the same token id with vanilla VQ-VAE. As a remedy, we introduce a group VQ-VAE to address this issue.

3 PRELIMINARY

Graph Neural Networks (GNNs) are the dominant tools for modeling graph data (Kipf & Welling, 2016; Velickovic et al., 2018; Hamilton et al., 2017; Xu et al., 2019). The structure of graph data guides the aggregation of local neighborhood information and leads to a more contextual representation for each node. Also, we can adopt a graph pooling operation (Mesquita et al., 2020) to get the representation for the whole graph. Let $\mathcal{G} = (\mathcal{V}, \mathcal{E})$ denotes a graph with node attributes x_v for $v \in \mathcal{V}$ and edge attributes e_{uv} for $(u, v) \in \mathcal{E}$. Formally, supposing that $h_v^{(l)}$ is the representation of node v at the l-th GNN layer and $\mathcal{N}(v)$ are all the neighbor nodes of node v, the update procedure from the $(l-1)$-th layer to the l-th layer is:

$$h_v^{(l)} = \text{COMBINE}\left(h_v^{(l-1)}, \text{AGGREGATE}\left(\left\{\left(h_v^{(l-1)}, h_u^{(l-1)}, e_{uv}\right) : u \in \mathcal{N}(v)\right\}\right)\right), \quad (1)$$

where e_{uv} denotes the edge between node u and v. $\text{AGGREGATE}(\cdot)$ is the aggregation function (e.g., mean operator) of the neighborhood information. $\text{COMBINE}(\cdot)$ combines the information of neighbours and node v (e.g., concatenation operator). After L iterations of message passing, the hidden states $h_v^{(L)}$ in the last iteration are the embeddings of v. Finally, we adopt a $\text{READOUT}(\cdot)$ operation (e.g., averaging, sum or graph pooling) to get the representation $\mathbf{h}_G$ for the whole graph G:

$$\mathbf{h}_G = \text{READOUT}\left(\left\{h_v^{(L)} \mid v \in \mathcal{V}\right\}\right). \quad (2)$$

4 PROPOSED PRE-TRAINING FRAMEWORK: MOLE-BERT

In this section, we will introduce the proposed pre-training framework Mole-BERT, which includes a node-level per-training approach (MAM) and a graph-level pre-training approach (TMCL).

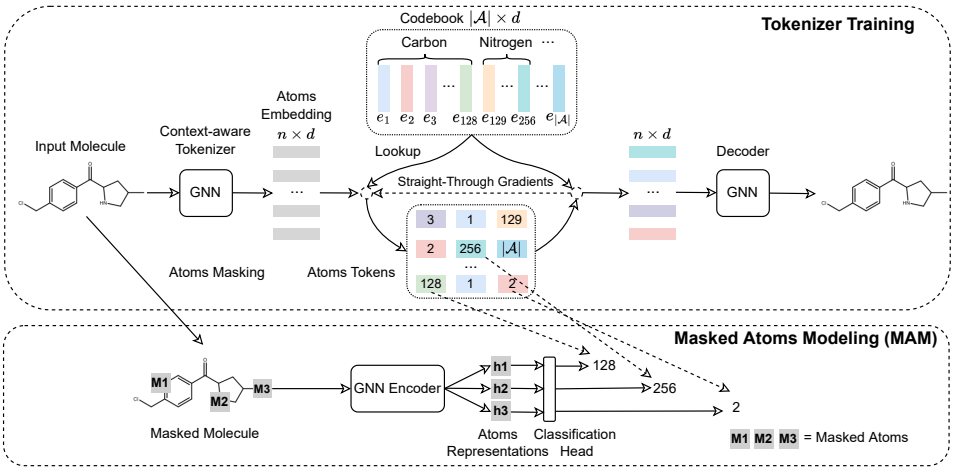

Figure 2: Schematic diagram of the tokenizer training and masked atoms modeling (MAM).

4.1 MASKED ATOMS MODELING (MAM)

Similar to NLP, we represent the atoms as discrete tokens using group VQ-VAE shown in Figure 2. Formally, the atoms $\mathcal{V} = \{v_1, v_2, \cdots, v_n\}$ of a molecule graph $\mathcal{G}$ is tokenized to $\boldsymbol{z} = \{z_1, z_2, \cdots, z_n\} \in \mathcal{A}^n$, where the atom vocabulary $\mathcal{A}$ contain $|\mathcal{A}|$ ($|\mathcal{A}| = 512$) discrete codes. Firstly, the GNN encoder of group VQ-VAE encodes the atoms to atoms embeddings. Next, the vector quantizer (VQ) looks up the nearest neighbor in the codebook for each atom embedding h_i. Let $\{e_1, e_2, \cdots, e_{|\mathcal{A}|}\}$ denote the codebook embeddings. The quantized code of the i-th atom is:

$$z_i = \text{argmin}_j \left\|h_i - e_j\right\|_2. \quad (3)$$

After quantizing the atoms to discrete tokens, we feed the corresponding codebook embeddings $\{e_{z_1}, e_{z_2}, \cdots, e_{z_n}\}$ to the decoder to reconstruct the input molecule graph. Kindly note that the vector quantization process is non-differentiable. In order to train the encoder, the gradient is approximated

like the straight-through estimator (Bengio et al., 2013) and copied from the decoder to the encoder. Intuitively, the quantizer looks up the nearest code for each encoder output, so the gradients of codebook embeddings can be utilized to train the encoder approximately. With the input attributes v_i and reconstructed attributes $\widehat{v_i}$, the training loss of the tokenizer for the molecule graph $\mathcal{G}$ is,

$$\mathcal{L}_{\texttt{VQ}} = \frac{1}{n}\sum_{i=1}^{n}\left(1 - \frac{v_i^T \widehat{v_i}}{\|v_i\| \cdot \|\widehat{v_i}\|}\right)^{\gamma} + \frac{1}{n}\sum_{i=1}^{n}\|\text{sg}[h_i] - e_{z_i}\|_2^2 + \frac{\beta}{n}\sum_{i=1}^{n}\|\text{sg}\left[e_{z_i}\right] - h_i\|_2^2, \quad (4)$$

where the first term is a reconstruction loss with the scaled cosine error ($\gamma \geq 1$), the second term is a VQ loss aiming to update the codebook and the third term is a commitment loss which encourages the output of the encoder to stay close to the chosen codebook embedding. $\text{sg}\left[\cdot\right]$ denotes stop-gradient, β is a hyper-parameter set to 0.25 in our experiments. This idea is inspired by DALL-E (Ramesh et al., 2021) which uses discrete VAE as a tokenizer for text-to-image generation. We show the superiority of our tokenizer over discrete VAE empirically in Appendix H and clarify the difference here: (1) Our tokenizer tokenizes atoms to discrete codes in a context-aware manner; (2) We use the tokens for pre-training instead of autoregressive generation; (3) We observe that atoms of different types might be allocated with the same token id with vanilla VQ-VAE. As a remedy, we introduce a group VQ-VAE to address this issue. Specifically, we divide the codebook embeddings into several groups, each of which corresponds to specific atom types. For example, the quantized codes of carbon, nitrogen and oxygen are restricted to $[1, 128]$, $[129, 256]$ and $[257, 384]$, respectively. The left rare atoms are restricted to $[385, 512]$ because they are less likely to conflict with each other. Additionally, we will release the tokenizer as an off-the-shelf tool for better or larger-scale molecular graph pre-training, just like what WordPiece (Wu et al., 2016) and BPE (Sennrich et al., 2015) have done for the NLP community. With the new tokenizer, we propose MAM to pre-train GNNs. Given an input molecule graph $\mathcal{G}$, we randomly mask its 15% atoms' tokens and pre-train GNNs to predict them. We study the influence of the masking ratios in Appendix C. We term the masked atoms' index set as $\mathcal{M}$ and the masked molecular graph as $\mathcal{G}^{\mathcal{M}}$. For each masked atom $i \in \mathcal{M}$, a softmax classifier is adopted to predict the discrete values over the vocabulary $\mathcal{A}$. The pre-training loss of MAM is:

$$\mathcal{L}_{\texttt{MAM}} = -\sum_{\mathcal{G}\in\mathcal{D}}\sum_{i\in\mathcal{M}}\log p\left(z_i \mid \mathcal{G}^{\mathcal{M}}\right), \quad (5)$$

where $\mathcal{D}$ denotes the datasets and z_i is the token of the atom v_i. Theoretically, we provide an explanation of MAM from the perspective of denoising variational autoencoder (Kingma & Welling, 2014). Given that $\widetilde{v_i}$ is the masked atom, The evidence lower bound (ELBO) of the log-likelihood is,

$$\sum_{\mathcal{G}\in\mathcal{D}}\sum_{i\in\mathcal{M}}\log p\left(v_i \mid \widetilde{v_i}\right) \geq \sum_{\mathcal{G}\in\mathcal{D}}\sum_{i\in\mathcal{M}}(\mathbb{E}_{z_i\sim q_\phi(\mathbf{z}|v_i)}\left[\log p_\psi\left(v_i \mid z_i\right)\right] - D_{\text{KL}}\left[q_\phi\left(\mathbf{z} \mid v_i\right) \| p_\theta\left(\mathbf{z} \mid \widetilde{v_i}\right)\right]), \quad (6)$$

where $q_\phi\left(z \mid v\right)$ is the encoder that outputs atoms tokens, $p_\psi\left(v \mid z\right)$ is the decoder that reconstructs the molecules given the tokens. Additionally, $p_\theta\left(z \mid \widetilde{v}\right)$ predicts the masked atoms' tokens given the corrupted molecules, which is the MAM pre-training task indeed. In the stage of tokenizer training, we minimize the graph reconstruction loss term. In the pre-training stage, the tokenizer q_ϕ and decoder p_ψ are fixed. Hence, we can simplify $q_\phi\left(\mathbf{z} \mid v\right)$ to an one-point distribution with the most likely atom tokens $\hat{z}_i = \arg\max_z q_\phi\left(z \mid v_i\right)$. Then the right side of Eq. (6) is,

$$\sum_{\mathcal{G}\in\mathcal{D}}\sum_{i\in\mathcal{M}}(\underbrace{\mathbb{E}_{z_i\sim q_\phi(z|v_i)}\left[\log p_\psi\left(v_i \mid z_i\right)\right]}_{\text{Stage 1: Tokenizer training (Graph Reconstruction)}} + \underbrace{\log p_\theta\left(\hat{z}_i \mid \widetilde{v_i}\right)}_{\text{Stage 2: Masked Atoms Modeling (MAM)}}), \quad (7)$$

which means that the joint objectives of tokenizer pre-training and MAM are maximizing the ELBO of the log-likelihood. Additionally, we study the time complexity of MAM in Appendix G.

4.2 Graph-level Task: Triplet Masked Contrastive Learning (TMCL)

Although MAM can mitigate the negative transfer issue, we observe that it fails to capture molecular graph-level semantics. Specifically, we first calculate the widely-used Tanimoto coefficient (Bajusz et al., 2015) of the extended connectivity fingerprints (ECFP) (Rogers & Hahn, 2010) between two molecules as their chemical similarity and pick the molecule pairs with top 15% similarity as 'similar' ones. All the molecule pairs in the datasets are 'random' pairs. Figure 4(a) shows significant inconsistency between the learned representations (by MAM) and

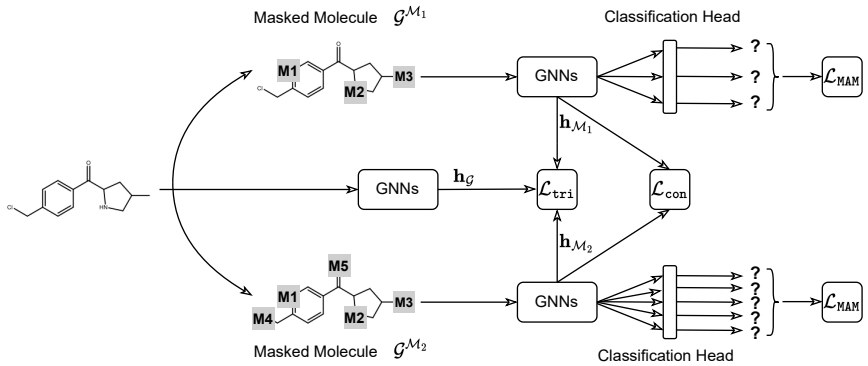

Figure 3: Schematic diagram of Mole-BERT.

ECFP, which will impair molecule retrieval using MAM (See Section 5.3) because two random molecules may have high similarity scores (lack of uniformity), while closely related molecules may have more different representations (lack of alignment) (Wang & Isola, 2020). On the other hand, existing graph-level pre-training tasks often follow a supervised paradigm (Hu et al., 2020), where the labels for molecules are expensive for the laborious wet-lab experiments. Graph contrastive learning (You et al., 2020) is a possible remedy for the above issues. For each molecule (anchor), they maximize the agreement between paired molecular graph augmentations (positive pairs) and push away other molecules in the batch as negative pairs (dissimilar molecules) indiscriminately. However, we argue that there are varying degrees of semantic similarity between molecules. For example, the similarity between formic acid (negative) and acetic acid (anchor) should be more significant than the one between ethanol (negative) and acetic acid (anchor). Previous contrastive approaches fail to model such partial order of semantic similarity. We introduce triplet masked contrastive learning, dubbed TMCL, to mitigate this crucial defect. More specifically, for each molecular graph $\mathcal{G}$, we first generate its augmented version $\mathcal{G}^{\mathcal{M}_1}$ with masked atoms index $\mathcal{M}_1$ and a smaller masking ratio (e.g., 15%). Then we enlarge the masking ratio (e.g., 30%) and obtain the other augmented version $\mathcal{G}^{\mathcal{M}_2}$ with atoms index $\mathcal{M}_2$. Now, we constitute a triplet $(\mathcal{G}, \mathcal{G}^{\mathcal{M}_1}, \mathcal{G}^{\mathcal{M}_2})$ with latent relation among them, i.e., $\mathcal{G}^{\mathcal{M}_1}$ is more similar to $\mathcal{G}$ than $\mathcal{G}^{\mathcal{M}_2}$ to $\mathcal{G}$. Although index $\mathcal{M}_1$ may lie in some crucial atom sets (e.g., functional group) that are indicative of molecular properties sometimes, the latent relation holds true in most cases and pre-training with abundant data will help alleviate this issue. Given that $\mathbf{h}_{\mathcal{G}}$, $\mathbf{h}_{\mathcal{M}_1}$, $\mathbf{h}_{\mathcal{M}_2}$ are the graph-level representations for $\mathcal{G}$, $\mathcal{G}^{\mathcal{M}_1}$ and $\mathcal{G}^{\mathcal{M}_2}$, respectively, we can formulate the triplet loss as,

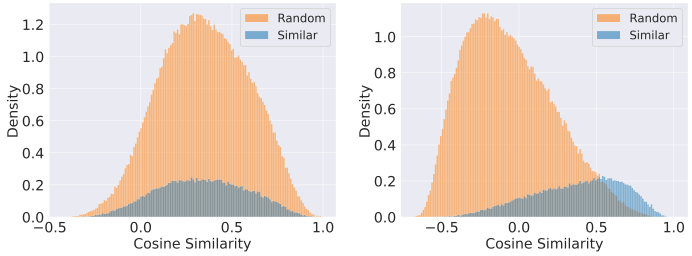

(a) MAM (b) MAM + TMCL (Mole-BERT)

Figure 4: Similarity histograms of MAM and Mole-BERT on Toxcast dataset. Cosine similarity measures the similarity between the learned representations while 'Random' and 'Similar' are defined with the chemical similarity between molecular fingerprints (ECFP). The histogram of GraphCL (You et al., 2020) can be seen in Appendix J.

$$\mathcal{L}_{\texttt{tri}} = \sum_{\mathcal{G}\in\mathcal{D}} \max\left(sim\left(\mathbf{h}_{\mathcal{G}}, \mathbf{h}_{\mathcal{M}_1}\right) - sim\left(\mathbf{h}_{\mathcal{G}}, \mathbf{h}_{\mathcal{M}_2}\right) + m, 0\right), \tag{8}$$

where $sim(\cdot,\cdot)$ denotes the cosine similarity and m is the margin. Now, we can combine the triplet loss $\mathcal{L}_{\texttt{tri}}$ with commonly-used contrastive loss $\mathcal{L}_{\texttt{con}}$ as graph-level pre-training objective $\mathcal{L}_{\texttt{TMCL}}$,

$$\mathcal{L}_{\texttt{TMCL}} = \mathcal{L}_{\texttt{con}} + \lambda\mathcal{L}_{\texttt{tri}}, \quad \text{where} \quad \mathcal{L}_{\texttt{con}} = -\sum_{\mathcal{G}\in\mathcal{D}} \log \frac{e^{sim(\mathbf{h}_{\mathcal{M}_1}, \mathbf{h}_{\mathcal{M}_2})/\tau}}{\sum_{\mathcal{G}'\in\mathcal{B}} e^{sim(\mathbf{h}_{\mathcal{M}_1}, \mathbf{h}_{\mathcal{G}'})/\tau}}, \tag{9}$$

$\mathcal{B}$ is the sampled batch including $\mathcal{G}$, and τ is the temperature hyper-parameter. Finally, MAM and TMCL constitute a unified pre-training framework, Mole-BERT (See Figure 3), whose hybrid loss is,

$$\mathcal{L}_{\texttt{Mole-BERT}} = \mathcal{L}_{\texttt{MAM}} + \mathcal{L}_{\texttt{TMCL}}. \tag{10}$$

5 EXPERIMENTS

5.1 DATASETS

For the pre-training stage, we use 2 million molecules sampled from the ZINC15 database (Sterling & Irwin, 2015) following previous works (Hu et al., 2020). The main downstream task is molecular property prediction, where we adopt the widely-used 8 binary classification datasets contained in MoleculeNet (Wu et al., 2018). Kindly note that we use *scaffold splitting* (Ramsundar et al., 2019), which splits the molecules according to their structures to mimic the real-world use cases. Additionally, we validate the effectiveness of Mole-BERT on a broader range of downstream tasks and datasets (See Section 5.3). The detailed information of all the datasets can be seen in Appendix A.

5.2 EXPERIMENTS CONFIGURATION

We use a 5-layer Graph Isomorphism Networks (GINs) whose hidden dimension is 300 (Xu et al., 2019) as the backbone architecture, which is one of the state-of-the-art GNNs for graph-level tasks. We adopt mean pooling as the readout function. During the pre-training stage, GNNs are pre-trained for 100 epochs with batch-size as 256 and the learning rate as 0.001. During the fine-tuning stage, we train for 100 epochs with batch-size as 32 and report the test score with the best cross-validation performance. The split for train/validation/test sets is $80\% : 10\% : 10\%$. The hyper-parameter λ is picked from $\{0.1, 0.3, 0.5\}$ with the validation set. All the experiments are conducted on Tesla V100 GPUs. Additionally, considering that previous works adopt different evaluation protocols, we reproduce all the results with the same protocol (10 random seeds + scaffold splitting) as the pioneering work (Hu et al., 2020) rigorously for fairness. *More details can be found in Appendix B.*

Table 1: Results for molecular property prediction (classification). We report the mean (standard deviation) ROC-AUC of 10 random seeds with scaffold splitting. The best results and the second best are highlighted with **bold** and bold, respectively. 'No pretrain' means training GNNs from scratch.

	Tox21	ToxCast	Sider	ClinTox	MUV	HIV	BBBP	Bace	Average
# Molecules	7,831	8,575	1,427	1,478	93,087	41,127	2,039	1,513	-
No pretrain	74.6 (0.4)	61.7 (0.5)	58.2 (1.7)	58.4 (6.4)	70.7 (1.8)	75.5 (0.8)	65.7 (3.3)	72.4 (3.8)	67.15
InfoGraph (Sun et al., 2020b)	73.3 (0.6)	61.8 (0.4)	58.7 (0.6)	75.4 (4.3)	74.4 (1.8)	74.2 (0.9)	68.7 (0.6)	74.3 (2.6)	70.10
EdgePred (Hamilton et al., 2017)	74.8 (0.6)	60.9 (0.5)	56.4 (1.3)	56.2 (8.1)	74.0 (1.9)	74.7 (0.5)	64.9 (5.6)	64.8 (3.5)	65.84
GPT-GNN (Hu & others., 2020)	74.9 (0.3)	62.5 (0.4)	58.1 (0.3)	58.3 (5.2)	75.9 (2.3)	65.2 (2.1)	64.5 (1.4)	77.9 (3.2)	68.45
ContextPred (Hu et al., 2020)	73.6 (0.3)	62.6 (0.6)	59.7 (1.8)	74.0 (3.4)	72.5 (1.5)	75.6 (1.0)	70.6 (1.5)	78.8 (1.2)	70.93
GraphLoG (Xu et al., 2021)	73.4 (0.6)	62.0 (0.6)	57.6 (1.9)	61.7 (2.6)	73.5 (1.6)	73.7 (1.1)	68.3 (1.6)	78.6 (1.0)	68.60
G-Contextual (Rong et al., 2020b)	75.0 (0.6)	62.8 (0.7)	58.7 (1.0)	60.6 (5.2)	72.1 (0.7)	76.3 (1.5)	69.9 (2.1)	79.3 (1.1)	69.34
G-Motif (Rong et al., 2020b)	73.6 (0.7)	62.3 (0.6)	61.0 (1.5)	77.7 (2.7)	73.0 (1.8)	73.8 (1.2)	66.9 (3.1)	73.0 (3.3)	70.16
AD-GCL (Suresh et al., 2021)	74.9 (0.4)	63.1 (0.7)	61.5 (0.9)	76.6 (2.8)	72.2 (1.7)	75.7 (1.1)	69.7 (0.5)	75.6 (1.0)	71.16
KCL (Fang et al., 2022b)	74.2 (0.6)	62.6 (0.5)	59.5 (0.7)	65.3 (5.2)	73.6 (2.3)	75.5 (0.7)	65.3 (1.0)	74.2 (1.3)	68.78
JOAO (You et al., 2021)	74.8 (0.6)	62.8 (0.7)	60.4 (1.5)	66.6 (3.1)	76.6 (1.7)	76.9 (0.7)	66.4 (1.0)	73.2 (1.6)	69.71
SimGRACE (Xia et al., 2022a)	74.4 (0.3)	62.6 (0.7)	60.2 (0.9)	75.5 (2.0)	75.4 (1.3)	75.0 (0.6)	71.2 (1.1)	74.9 (2.0)	71.15
GraphCL (You et al., 2020)	75.1 (0.7)	63.0 (0.4)	59.8 (1.3)	77.5 (3.8)	76.4 (0.4)	75.1 (0.7)	67.8 (2.4)	74.6 (2.1)	71.16
3D InfoMax (Stärk et al., 2022)	74.5 (0.7)	63.5 (0.8)	56.8 (2.1)	62.7 (3.3)	76.2 (1.4)	76.1 (1.3)	69.1 (1.2)	78.6 (1.9)	69.69
GraphMAE (Hou et al., 2022)	75.2 (0.9)	63.6 (0.3)	60.5 (1.2)	73.5 (3.0)	76.6 (2.0)	75.8 (0.6)	71.2 (1.0)	76.2 (1.9)	71.33
GraphMVP (Liu et al., 2022a)	74.9 (0.8)	63.1 (0.2)	60.2 (1.1)	**79.1** (2.8)	77.7 (0.6)	76.0 (0.1)	70.8 (0.5)	79.3 (1.5)	72.64
MGSSL (Zhang et al., 2021)	75.2 (0.6)	63.3 (0.5)	61.6 (1.0)	77.1 (4.5)	77.6 (0.4)	75.8 (0.4)	68.8 (0.6)	78.8 (0.9)	72.28
AttrMask (Hu et al., 2020)	75.1 (0.9)	63.3 (0.6)	60.5 (0.9)	73.5 (4.3)	75.8 (1.0)	75.3 (1.5)	65.2 (1.4)	77.8 (1.8)	70.81
MAM (with vanilla VQ-VAE)	75.8 (0.6)	63.1 (0.5)	60.7 (1.5)	74.2 (2.7)	76.5 (1.6)	76.2 (0.9)	66.4 (0.7)	78.2 (0.8)	71.39
TMCL (w/o $\mathcal{L}_{\texttt{con}}$)	73.5 (1.0)	61.8 (0.3)	58.7 (1.6)	61.1 (4.1)	71.6 (1.3)	73.5 (1.3)	65.4 (2.6)	73.7 (2.4)	67.41
TMCL (w/o $\mathcal{L}_{\texttt{tri}}$)	74.1 (0.4)	62.4 (0.8)	58.7 (3.0)	75.6 (2.2)	75.7 (1.1)	74.6 (1.1)	66.8 (1.4)	74.2 (1.3)	70.26
MAM	76.2 (0.5)	63.9 (0.3)	61.4 (1.9)	75.1 (3.0)	77.4 (2.1)	77.5 (1.0)	66.8 (1.5)	78.9 (1.1)	72.16
TMCL	74.9 (0.7)	63.2 (0.7)	59.6 (1.4)	77.0 (4.2)	77.2 (0.3)	75.3 (1.1)	67.6 (1.3)	75.1 (1.2)	71.24
Mole-BERT (MAM + TMCL)	**76.8** (0.5)	**64.3** (0.2)	**62.8** (1.1)	78.9 (3.0)	**78.6** (1.8)	**78.2** (0.8)	**71.9** (1.6)	**80.8** (1.4)	**74.04**

5.3 RESULTS AND ANALYSIS

Primary Results and Analysis. We document the main results of molecular property prediction in Table 1 and Table 2. Our systematic study suggests the following trends:
Observation I: The pre-training task of AttrMask incurs negative transfer issue on some datasets (HIV and BBBP). In contrast, MAM achieves consistent and notable improvements over AttrMask and 'No pretrain', although MAM pre-trains GNNs only with a node-level task. This observation verifies that only node-level pre-training tasks can also mitigate the negative transfer, which overturns the previous belief that pre-training GNNs at the level of individual nodes may give limited improvements. The reasons why AttrMask fails lie in the extremely small and unbalanced atoms vocabulary.
Observation II: Mole-BERT can achieve competitive or better performance than previous pre-training strategies under the same experimental protocols. More specifically, Mole-BERT outperforms 'No pretrain' model by 6.36% and the current state-of-the-art method GraphMVP by nearly 1.34%, though GraphMVP pre-trains GNNs on another molecular dataset with 3D geometry. To further support the above claims, we plot the training and testing accuracy curves in Appendix I.
Observation III: As demonstrated in Table 2, MAM can serve as a fundamental pre-training sub-task like AttrMask. Furthermore, MAM shows significant superiority over AttrMask when they serve as sub-tasks for multi-task GNNs pre-training.
Observation IV (Ablation Study): We substitute or remove some components of the proposed approaches to study their effectiveness. As can be observed in Table 1, the group VQ-VAE is superior to vanilla VQ-VAE in MAM because it prevents the atoms of different types be allocated with the same token id. Additionally, we observe a notable performance drop when we remove the triplet loss $\mathcal{L}_{\texttt{tri}}$ or contrastive loss $\mathcal{L}_{\texttt{con}}$ in TMCL, which indicates both of them are necessary and effective.

Table 2: Performance of AttrMask and MAM when they serve as fundamental pre-training sub-tasks. The data for supervised pre-training (Hu et al., 2020) comes from a preprocessed ChEMBL dataset (Gaulton et al., 2012a) with some labels from biochemical assays.

	Tox21	ToxCast	Sider	ClinTox	MUV	HIV	BBBP	Bace	Average
MGSSL (AttrMask)	75.2 (0.6)	63.3 (0.5)	61.6 (1.0)	77.1 (4.5)	77.6 (0.4)	75.8 (0.4)	68.8 (0.6)	78.8 (0.9)	72.28
MGSSL (MAM)	76.6 (0.7)	64.5 (0.9)	62.1 (0.8)	78.2 (3.8)	78.7 (0.5)	76.9 (0.7)	70.5 (1.1)	80.2 (1.5)	**73.46**
Supervised (Hu et al., 2020)	76.8 (0.8)	65.2 (0.5)	61.7 (0.8)	57.0 (2.8)	79.8 (1.6)	74.3 (1.5)	67.9 (0.9)	77.7 (0.8)	70.05
Supervised + AttrMask	77.8 (0.6)	65.3 (0.8)	63.2 (0.8)	73.8 (3.6)	80.9 (1.6)	77.5 (1.3)	66.8 (1.4)	80.7 (1.3)	73.25
Supervised + MAM	78.6 (0.5)	66.9 (0.4)	64.0 (1.0)	75.4 (2.9)	81.8 (1.6)	78.8 (1.0)	69.1 (1.7)	82.3 (1.2)	**74.61**

Influence of GNNs Backbone. As shown in Table 3, we verify that Mole-BERT is agnostic to the GNN architectures by trying four popular GNN models including GIN (Xu et al., 2019), GCN (Kipf. & Welling, 2017), R-GCN (Schlichtkrull et al., 2018) and GraphSAGE (Hamilton et al., 2017). As can be observed, Mole-BERT achieves consistent and notable improvements over training from scratch with various GNNs. Additionally, pre-training with GIN achieves the most significant gains.

Table 3: Compare pre-training gains (averaged ROC-AUC (%) on 8 datasets) with different GNN architectures. The relative gains mean the relative improvements of Mole-BERT over 'No pre-train'.

Model	GCN	GIN	R-GCN	GraphSAGE
No pretrain	68.77	67.15	68.32	68.46
MAM	71.35	72.16	70.76	71.55
TMCL	68.93	71.24	69.25	69.58
Mole-BERT	73.22	74.04	73.51	73.74
Relative gain	+6.47 %	+10.26 %	+7.60 %	+7.71 %

Broader Range of Downstream Tasks. We report the performance in regressive property prediction and Drug-target affinity (DTA) tasks in Table 4. DTA is a crucial task in drug discovery, where we aim to predict the affinity scores between the molecular drugs and protein targets. We follow the settings of a recent work (Nguyen et al., 2021) on DTA which models the molecular graphs with GNN and target protein (as an amino-acid sequence) with a convolution neural network (CNN). We substitute the GNN in their approach with pre-trained GNNs. The superior performance indicates that Mole-BERT can work well in a broader range of downstream tasks.

Table 4: Results for molecular property prediction (regression) and DTA (regression). We report the mean (and standard variance) RMSE of 3 seeds with scaffold splitting for molecular property prediction, and the mean (and standard variance) MSE for 3 seeds with random splitting on DTA tasks. *Both indicators are the less the better.* The best result for each task is highlighted in **bold**.

	Molecular Property Prediction (↓)				Drug-Target Affinity (↓)	
Datasets	ESOL	Lipo	Malaria	CEP	Davis	KIBA
No Pre-train	1.178 (0.044)	0.744 (0.007)	1.127 (0.003)	1.254 (0.030)	0.286 (0.006)	0.206 (0.004)
ContextPred	1.196 (0.037)	0.702 (0.020)	1.101 (0.015)	1.243 (0.025)	0.279 (0.002)	0.198 (0.004)
JOAO	1.120 (0.019)	0.708 (0.007)	1.145 (0.010)	1.293 (0.003)	0.281 (0.004)	0.196 (0.005)
GraphMVP	1.064 (0.045)	0.691 (0.013)	1.106 (0.013)	**1.228** (0.001)	0.274 (0.002)	0.175 (0.001)
AttrMask	1.112 (0.048)	0.730 (0.004)	1.119 (0.014)	1.256 (0.000)	0.291 (0.007)	0.203 (0.003)
MAM	1.098 (0.025)	0.711 (0.010)	1.107 (0.009)	1.240 (0.006)	0.278 (0.005)	0.188 (0.007)
TMCL	1.116 (0.042)	0.704 (0.014)	1.123 (0.017)	1.262 (0.011)	0.282 (0.005)	0.194 (0.002)
Mole-BERT	**1.015** (0.030)	**0.676** (0.017)	**1.074** (0.009)	1.232 (0.009)	**0.266** (0.004)	**0.157** (0.001)

Table 5: The performance with various vocabulary sizes on 8 MoleculeNet datasets.

Vocabulary size	128	256	512	1, 024	2, 048
MAM	71.42	71.65	72.16	**72.21**	71.66
Mole-BERT	73.23	73.56	**74.04**	74.02	73.86

Influence of the Vocabulary Size. In our previous experiments, we set the vocabulary size as 512. However, we cannot decide the optimal vocabulary size for MAM because the exact atoms sub-types are unavailable. In Table 5, we study the vocabulary size ranging from 128 to 2,048, from which we can observe: **(1)** Even if when we set the vocabulary size as 128, near 119 of AttrMask, MAM can outperform AttrMask by a significant margin, which indicates that the tokens derived by VQ-VAE are context-aware and is superior to pure atoms' identities; **(2)** Vocabulary size also influence on MAM's performance. Although the vocabulary size of 1, 024 outperforms 512, the superiority is not significant. Hence, we set 512 as the default vocabulary size considering the computational budget.

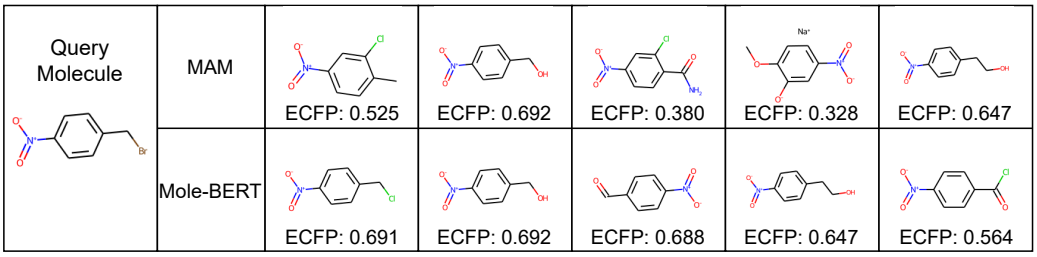

Figure 5: The query molecule and 5 closest molecules with the extracted representations.

Molecule Retrieval. For more comprehensive evaluations, we first extract the representation for a query molecule. And then, we calculate its cosine similarities with all reference molecules in ToxCast dataset. We demonstrate 5 molecules that are most similar to the query molecule with the cosine similarities in Figure 5. As can be observed, the representation similarities of Mole-BERT are approximately aligned with the fingerprint similarities, which indicates that Mole-BERT learns chemically meaningful representations. Moreover, the representations extracted from MAM fail to model the varying degree of similarities between molecules. Hence, graph-level tasks like TMCL are necessary and effective for molecule retrieval. More ablations and results can be seen in Appendix E.

6 Conclusions and Future Works.

In this paper, we find the negative transfer issue of AttrMask can be attributed to the extremely small and unbalanced atom vocabulary. As a remedy, we contribute a context-aware tokenizer with group VQ-VAE. With the new vocabulary, we propose a more suitable pre-training task, MAM, to mitigate the negative transfer issue of AttrMask. Additionally, we develop triplet masked contrastive learning (TMCL) to model the varying degree of molecular similarities. MAM and TMCL constitute a joint pre-training framework (Mole-BERT), which achieves superior performance over state-of-the-art methods while not requiring any domain knowledge. For the future, it remains to be explored whether the proposed pre-training strategies can be applied to SMILES (Weininger et al., 1989) sequence-based molecular pre-training, where small and unbalanced vocabulary also impairs performance.

REFERENCES

Tox21 challenge. *https://tripod.nih.gov/tox21/challenge/*, 2017.

Dávid Bajusz, Anita Rácz, and Károly Héberger. Why is tanimoto index an appropriate choice for fingerprint-based similarity calculations? *Journal of cheminformatics*, 7(1):1–13, 2015.

Hangbo Bao, Li Dong, Furu Wei, Wenhui Wang, Nan Yang, Xiaodong Liu, Yu Wang, Jianfeng Gao, Songhao Piao, Ming Zhou, et al. Unilmv2: Pseudo-masked language models for unified language model pre-training. In *International Conference on Machine Learning*, pp. 642–652. PMLR, 2020.

Hangbo Bao, Li Dong, and Furu Wei. Beit: Bert pre-training of image transformers. *arXiv preprint arXiv:2106.08254*, 2021.

Yoshua Bengio, Nicholas Léonard, and Aaron Courville. Estimating or propagating gradients through stochastic neurons for conditional computation. *arXiv preprint arXiv:1308.3432*, 2013.

Mark Chen, Alec Radford, Rewon Child, Jeffrey Wu, Heewoo Jun, David Luan, and Ilya Sutskever. Generative pretraining from pixels. In *International conference on machine learning*, pp. 1691–1703. PMLR, 2020.

Kevin Clark, Minh-Thang Luong, Quoc V. Le, and Christopher D. Manning. ELECTRA: Pre-training text encoders as discriminators rather than generators. In *ICLR*, 2020. URL `https://openreview.net/pdf?id=r1xMH1BtvB`.

Mindy I Davis, Jeremy P Hunt, Sanna Herrgard, Pietro Ciceri, Lisa M Wodicka, Gabriel Pallares, Michael Hocker, Daniel K Treiber, and Patrick P Zarrinkar. Comprehensive analysis of kinase inhibitor selectivity. *Nature biotechnology*, 29(11):1046–1051, 2011.

John S Delaney. Esol: estimating aqueous solubility directly from molecular structure. *Journal of chemical information and computer sciences*, 2004.

Jacob Devlin, Ming-Wei Chang, and others. Bert: Pre-training of deep bidirectional transformers for language understanding. *NAACL*, 2019.

Alexey Dosovitskiy, Lucas Beyer, Alexander Kolesnikov, Dirk Weissenborn, Xiaohua Zhai, Thomas Unterthiner, Mostafa Dehghani, Matthias Minderer, Georg Heigold, Sylvain Gelly, Jakob Uszkoreit, and Neil Houlsby. An image is worth 16x16 words: Transformers for image recognition at scale. In *International Conference on Learning Representations*, 2021. URL `https://openreview.net/forum?id=YicbFdNTTy`.

Xiaomin Fang, Lihang Liu, Jieqiong Lei, Donglong He, Shanzhuo Zhang, Jingbo Zhou, Fan Wang, Hua Wu, and Haifeng Wang. Geometry-enhanced molecular representation learning for property prediction. *Nature Machine Intelligence*, 4(2):127–134, 2022a.

Yin Fang, Qiang Zhang, Haihong Yang, Xiang Zhuang, Shumin Deng, Wen Zhang, Ming Qin, Zhuo Chen, Xiaohui Fan, and Huajun Chen. Molecular contrastive learning with chemical element knowledge graph. In *Proceedings of the Thirty-Sixth AAAI Conference on Artificial Intelligence (AAAI)*, 2022b.

Francisco-Javier Gamo, Laura M Sanz, Jaume Vidal, Cristina De Cozar, Emilio Alvarez, Jose-Luis Lavandera, Dana E Vanderwall, Darren VS Green, Vinod Kumar, Samiul Hasan, et al. Thousands of chemical starting points for antimalarial lead identification. *Nature*, 465(7296):305, 2010.

Anna Gaulton, Louisa J. Bellis, A. Patrícia Bento, Jon Chambers, Mark Davies, Anne Hersey, Yvonne Light, Shaun McGlinchey, David Michalovich, Bissan Al-Lazikani, and John P. Overington. Chembl: a large-scale bioactivity database for drug discovery. *Nucleic Acids Research*, 2012a.

Anna Gaulton, Louisa J Bellis, A Patricia Bento, Jon Chambers, Mark Davies, Anne Hersey, Yvonne Light, Shaun McGlinchey, David Michalovich, Bissan Al-Lazikani, et al. Chembl: a large-scale bioactivity database for drug discovery. *Nucleic acids research*, 40(D1):D1100–D1107, 2012b.

Kaitlyn M Gayvert, Neel S Madhukar, and Olivier Elemento. A data-driven approach to predicting successes and failures of clinical trials. *Cell chemical biology*, 2016.

Johannes Hachmann, Roberto Olivares-Amaya, Sule Atahan-Evrenk, Carlos Amador-Bedolla, Roel S Sánchez-Carrera, Aryeh Gold-Parker, Leslie Vogt, Anna M Brockway, and Alán Aspuru-Guzik. The harvard clean energy project: large-scale computational screening and design of organic photovoltaics on the world community grid. *The Journal of Physical Chemistry Letters*, 2(17): 2241–2251, 2011.

Will Hamilton, Zhitao Ying, and Jure Leskovec. Inductive representation learning on large graphs. *Advances in neural information processing systems*, 30, 2017.

Kaiming He, Xinlei Chen, Saining Xie, Yanghao Li, Piotr Dollár, and Ross Girshick. Masked autoencoders are scalable vision learners. In *Proceedings of the IEEE/CVF Conference on Computer Vision and Pattern Recognition*, pp. 16000–16009, 2022.

Zhenyu Hou, Xiao Liu, Yukuo Cen, Yuxiao Dong, Hongxia Yang, Chunjie Wang, and Jie Tang. Graphmae: Self-supervised masked graph autoencoders. *arXiv e-prints*, pp. arXiv–2205, 2022.

Weihua Hu, Bowen Liu, and others. Strategies for pre-training graph neural networks. *ICLR*, 2020.

Ziniu Hu and others. Gpt-gnn: Generative pre-training of graph neural networks. *KDD*, 2020.

Mandar Joshi, Danqi Chen, Yinhan Liu, Daniel S Weld, Luke Zettlemoyer, and Omer Levy. Spanbert: Improving pre-training by representing and predicting spans. *Transactions of the Association for Computational Linguistics*, 8:64–77, 2020.

Diederik P. Kingma and Max Welling. Auto-Encoding Variational Bayes. In *2nd International Conference on Learning Representations, ICLR 2014, Banff, AB, Canada, April 14-16, 2014, Conference Track Proceedings*, 2014.

N. Thomas Kipf. and M. Welling. Semi-supervised classification with graph convolutional networks. *ICLR*, 2017.

Thomas N Kipf and Max Welling. Variational graph auto-encoders. *arXiv preprint arXiv:1611.07308*, 2016.

Matej Kosec, Sheng Fu, and Mario Michael Krell. Packing: Towards 2x nlp bert acceleration. *arXiv preprint arXiv:2107.02027*, 2021.

Michael Kuhn, Ivica Letunic, Lars Juhl Jensen, and Peer Bork. The sider database of drugs and side effects. *Nucleic acids research*, 44(D1):D1075–D1079, 2015.

Greg Landrum et al. Rdkit: A software suite for cheminformatics, computational chemistry, and predictive modeling, 2013.

Mike Lewis, Yinhan Liu, Naman Goyal, Marjan Ghazvininejad, Abdelrahman Mohamed, Omer Levy, Ves Stoyanov, and Luke Zettlemoyer. Bart: Denoising sequence-to-sequence pre-training for natural language generation, translation, and comprehension. *arXiv preprint arXiv:1910.13461*, 2019.

Pengyong Li, Jun Wang, and others. An effective self-supervised framework for learning expressive molecular global representations to drug discovery. *BIB*, 2021a.

Pengyong Li, Jun Wang, Yixuan Qiao, Hao Chen, Yihuan Yu, Xiaojun Yao, Peng Gao, Guotong Xie, and Sen Song. An effective self-supervised framework for learning expressive molecular global representations to drug discovery. *Briefings in Bioinformatics*, 22(6):bbab109, 2021b.

Zhaowen Li, Zhiyang Chen, Fan Yang, Wei Li, Yousong Zhu, Chaoyang Zhao, Rui Deng, Liwei Wu, Rui Zhao, Ming Tang, et al. Mst: Masked self-supervised transformer for visual representation. *Advances in Neural Information Processing Systems*, 34:13165–13176, 2021c.

Shengchao Liu, Hanchen Wang, Weiyang Liu, Joan Lasenby, Hongyu Guo, and Jian Tang. Pre-training molecular graph representation with 3d geometry. In *International Conference on Learning Representations*, 2022a. URL `https://openreview.net/forum?id=xQUe1pOKPam`.

Yinhan Liu, Myle Ott, Naman Goyal, Jingfei Du, Mandar Joshi, Danqi Chen, Omer Levy, Mike Lewis, Luke Zettlemoyer, and Veselin Stoyanov. Roberta: A robustly optimized bert pretraining approach. *arXiv preprint arXiv:1907.11692*, 2019.

Yixin Liu, Ming Jin, Shirui Pan, Chuan Zhou, Yu Zheng, Feng Xia, and Philip Yu. Graph self-supervised learning: A survey. *IEEE Transactions on Knowledge and Data Engineering*, 2022b.

Ines Filipa Martins, Ana L Teixeira, Luis Pinheiro, and Andre O Falcao. A bayesian approach to in silico blood-brain barrier penetration modeling. *Journal of chemical information and modeling*, 52 (6):1686–1697, 2012.

Diego Mesquita, Amauri Souza, and Samuel Kaski. Rethinking pooling in graph neural networks. *Advances in Neural Information Processing Systems*, 33:2220–2231, 2020.

Thin Nguyen, Hang Le, Thomas P Quinn, Tri Nguyen, Thuc Duy Le, and Svetha Venkatesh. Graphdta: Predicting drug–target binding affinity with graph neural networks. *Bioinformatics*, 37 (8):1140–1147, 2021.

Hakime Öztürk, Arzucan Özgür, and Elif Ozkirimli. Deepdta: deep drug–target binding affinity prediction. *Bioinformatics*, 34(17):i821–i829, 2018.

Jiezhong Qiu, Qibin Chen, Yuxiao Dong, Jing Zhang, Hongxia Yang, Ming Ding, Kuansan Wang, and Jie Tang. Gcc: Graph contrastive coding for graph neural network pre-training. In *Proceedings of the 26th ACM SIGKDD International Conference on Knowledge Discovery & Data Mining*, pp. 1150–1160, 2020.

Colin Raffel, Noam Shazeer, Adam Roberts, Katherine Lee, Sharan Narang, Michael Matena, Yanqi Zhou, Wei Li, Peter J Liu, et al. Exploring the limits of transfer learning with a unified text-to-text transformer. *J. Mach. Learn. Res.*, 21(140):1–67, 2020.

Aditya Ramesh, Mikhail Pavlov, Gabriel Goh, Scott Gray, Chelsea Voss, Alec Radford, Mark Chen, and Ilya Sutskever. Zero-shot text-to-image generation. In *International Conference on Machine Learning*, pp. 8821–8831. PMLR, 2021.

Bharath Ramsundar, Peter Eastman, Patrick Walters, and Vijay Pande. *Deep learning for the life sciences: applying deep learning to genomics, microscopy, drug discovery, and more*. O'Reilly Media, 2019.

Joshua David Robinson, Ching-Yao Chuang, Suvrit Sra, and Stefanie Jegelka. Contrastive learning with hard negative samples. In *International Conference on Learning Representations*, 2021. URL `https://openreview.net/forum?id=CR1XOQ0UTh-`.

David Rogers and Mathew Hahn. Extended-connectivity fingerprints. *Journal of chemical information and modeling*, 50(5):742–754, 2010.

Sebastian G Rohrer and Knut Baumann. Maximum unbiased validation (muv) data sets for virtual screening based on pubchem bioactivity data. *Journal of chemical information and modeling*, 49 (2):169–184, 2009.

Yu Rong, Yatao Bian, and others. Self-supervised graph transformer on large-scale molecular data. *NIPS*, 2020a.

Yu Rong, Yatao Bian, Tingyang Xu, Weiyang Xie, Ying Wei, Wenbing Huang, and Junzhou Huang. Self-supervised graph transformer on large-scale molecular data. *Advances in Neural Information Processing Systems*, 33:12559–12571, 2020b.

Lars Ruddigkeit, Ruud Van Deursen, Lorenz C Blum, and Jean-Louis Reymond. Enumeration of 166 billion organic small molecules in the chemical universe database gdb-17. *Journal of chemical information and modeling*, 52(11):2864–2875, 2012.

Michael Schlichtkrull, Thomas N Kipf, Peter Bloem, Rianne van den Berg, Ivan Titov, and Max Welling. Modeling relational data with graph convolutional networks. In *European semantic web conference*, pp. 593–607. Springer, 2018.

Rico Sennrich, Barry Haddow, and Alexandra Birch. Neural machine translation of rare words with subword units. *arXiv preprint arXiv:1508.07909*, 2015.

Hannes Stärk, Dominique Beaini, Gabriele Corso, Prudencio Tossou, Christian Dallago, Stephan Günnemann, and Pietro Liò. 3d infomax improves gnns for molecular property prediction. In *International Conference on Machine Learning*, pp. 20479–20502. PMLR, 2022.

T. Sterling and John J. Irwin. Zinc 15 – ligand discovery for everyone. *Journal of Chemical Information and Modeling*, 55:2324 – 2337, 2015.

Hannes Stärk, Dominique Beaini, Gabriele Corso, Prudencio Tossou, Christian Dallago, Stephan Günnemann, and Pietro Liò. 3d infomax improves gnns for molecular property prediction. *arXiv preprint arXiv:2110.04126*, 2021.

Fan-Yun Sun, Jordan Hoffman, Vikas Verma, and Jian Tang. Infograph: Unsupervised and semi-supervised graph-level representation learning via mutual information maximization. In *International Conference on Learning Representations*, 2020a. URL `https://openreview.net/forum?id=r1lfF2NYvH`.

Fan-Yun Sun, Jordan Hoffmann, and others. Infograph: Unsupervised and semi-supervised graph-level representation learning via mutual information maximization. *ICLR*, 2020b.

Mengying Sun, Jing Xing, and others. Mocl: Contrastive learning on molecular graphs with multi-level domain knowledge. *KDD*, 2021.

Susheel Suresh, Pan Li, Cong Hao, and Jennifer Neville. Adversarial graph augmentation to improve graph contrastive learning. *Advances in Neural Information Processing Systems*, 34, 2021.

Jing Tang, Agnieszka Szwajda, Sushil Shakyawar, Tao Xu, Petteri Hintsanen, Krister Wennerberg, and Tero Aittokallio. Making sense of large-scale kinase inhibitor bioactivity data sets: a comparative and integrative analysis. *Journal of Chemical Information and Modeling*, 54(3):735–743, 2014.

Shantanu Thakoor, Corentin Tallec, Mohammad Gheshlaghi Azar, Mehdi Azabou, Eva L Dyer, Remi Munos, Petar Veličković, and Michal Valko. Large-scale representation learning on graphs via bootstrapping. In *International Conference on Learning Representations*, 2022. URL `https://openreview.net/forum?id=0UXT6PpRpW`.

Aaron Van Den Oord, Oriol Vinyals, et al. Neural discrete representation learning. *Advances in neural information processing systems*, 30, 2017.

Petar Velickovic, Guillem Cucurull, Arantxa Casanova, Adriana Romero, Pietro Liò, and Yoshua Bengio. Graph attention networks. In *ICLR (Poster)*, 2018.

Petar Velickovic, William Fedus, William L Hamilton, Pietro Liò, Yoshua Bengio, and R Devon Hjelm. Deep graph infomax. In *ICLR (Poster)*, 2019.

Tongzhou Wang and Phillip Isola. Understanding contrastive representation learning through alignment and uniformity on the hypersphere. In *International Conference on Machine Learning*, pp. 9929–9939. PMLR, 2020.

Yuyang Wang, Jianren Wang, Zhonglin Cao, and Amir Barati Farimani. Molecular contrastive learning of representations via graph neural networks. *Nature Machine Intelligence*, 4(3):279–287, 2022.

Chen Wei, Haoqi Fan, Saining Xie, Chao-Yuan Wu, Alan Yuille, and Christoph Feichtenhofer. Masked feature prediction for self-supervised visual pre-training. In *Proceedings of the IEEE/CVF Conference on Computer Vision and Pattern Recognition*, pp. 14668–14678, 2022.

David Weininger, Arthur Weininger, and others. Smiles. 2. algorithm for generation of unique smiles notation. *J CHEM INF MODEL*, 1989.

Yonghui Wu, Mike Schuster, Zhifeng Chen, Quoc V Le, Mohammad Norouzi, Wolfgang Macherey, Maxim Krikun, Yuan Cao, Qin Gao, Klaus Macherey, et al. Google's neural machine translation system: Bridging the gap between human and machine translation. *arXiv preprint arXiv:1609.08144*, 2016.

Zhenqin Wu, Bharath Ramsundar, Evan N Feinberg, Joseph Gomes, Caleb Geniesse, Aneesh S Pappu, Karl Leswing, and Vijay Pande. Moleculenet: a benchmark for molecular machine learning. *Chemical science*, 9(2):513–530, 2018.

Jun Xia, Lirong Wu, , Jintao Chen, Bozhen Hu, and Stan Z. Li. SimGRACE: A Simple Framework for Graph Contrastive Learning without Data Augmentation. In *Proceedings of The Web Conference 2022*. Association for Computing Machinery, 2022a.

Jun Xia, Yanqiao Zhu, Yuanqi Du, and Stan Z. Li. Pre-training graph neural networks for molecular representations: Retrospect and prospect. In *ICML 2022 2nd AI for Science Workshop*, 2022b. URL https://openreview.net/forum?id=dhXLkrY2Nj3.

Yaochen Xie, Zhao Xu, Jingtun Zhang, Zhengyang Wang, and Shuiwang Ji. Self-supervised learning of graph neural networks: A unified review. *IEEE Transactions on Pattern Analysis and Machine Intelligence*, 2022.

Keyulu Xu, Weihua Hu, and others. How powerful are graph neural networks? In *ICLR*, 2019.

Minghao Xu, Hang Wang, Bingbing Ni, Hongyu Guo, and Jian Tang. Self-supervised graph-level representation learning with local and global structure. In *International Conference on Machine Learning*, pp. 11548–11558. PMLR, 2021.

Zhilin Yang, Zihang Dai, Yiming Yang, Jaime Carbonell, Russ R Salakhutdinov, and Quoc V Le. Xlnet: Generalized autoregressive pretraining for language understanding. *Advances in neural information processing systems*, 32, 2019.

Y. You, T. Chen, and others. Graph contrastive learning with augmentations. In *NeurIPS*, 2020.

Yuning You, Tianlong Chen, and others. Graph contrastive learning automated. *ICML*, 2021.

Daniel Zaharevitz. Aids antiviral screen data, 2015.

Zaixi Zhang, Qi Liu, and others. Motif-based graph self-supervised learning for molecular property prediction. *NeurIPS*, 2021.

Jinhua Zhu, Yingce Xia, Lijun Wu, Shufang Xie, Tao Qin, Wengang Zhou, Houqiang Li, and Tie-Yan Liu. Unified 2d and 3d pre-training of molecular representations. In *Proceedings of the 28th ACM SIGKDD Conference on Knowledge Discovery and Data Mining*, pp. 2626–2636, 2022.

Yanqiao Zhu, Yichen Xu, Qiang Liu, and Shu Wu. An empirical study of graph contrastive learning. In *Thirty-fifth Conference on Neural Information Processing Systems Datasets and Benchmarks Track (Round 2)*, 2021a. URL https://openreview.net/forum?id=UuUbIYnHKO.

Yanqiao Zhu, Yichen Xu, Feng Yu, Qiang Liu, Shu Wu, and Liang Wang. Graph contrastive learning with adaptive augmentation. In *Proceedings of the Web Conference 2021*, pp. 2069–2080, 2021b.

A DATASETS

In this section, we provide detailed information of the datasets used for downstream tasks.

Molecular Property: Pharmacology The Blood-Brain Barrier Penetration (BBBP) (Martins et al., 2012) dataset measures whether a molecule will penetrate the central nervous system. All three datasets, Tox21 (tox, 2017), ToxCast (Wu et al., 2018), and ClinTox (Gayvert et al., 2016) are related to the toxicity of molecular compounds. The Side Effect Resource (SIDER) (Kuhn et al., 2015) dataset stores the adverse drug reactions on a marketed drug database.

Molecular Property: Physical Chemistry Dataset proposed in (Delaney, 2004) measures aqueous solubility of the molecular compounds. Lipophilicity (Lipo) dataset is a subset of ChEMBL (Gaulton et al., 2012b) measuring the molecule octanol/water distribution coefficient. CEP dataset is a subset of the Havard Clean Energy Project (CEP) (Hachmann et al., 2011), which estimates the organic photovoltaic efficiency.

Molecular Property: Biophysics Maximum Unbiased Validation (MUV) (Rohrer & Baumann, 2009) is another sub-database from PCBA, and is obtained by applying a refined nearest neighbor analysis. HIV is from the Drug Therapeutics Program (DTP) AIDS Antiviral Screen (Zaharevitz, 2015), and it aims at predicting inhibit HIV replication. BACE measures the binding results for a set of inhibitors of β-secretase 1 (BACE-1) and is gathered in MoleculeNet (Wu et al., 2018). Malaria (Gamo et al., 2010) measures the drug efficacy against the parasite that causes malaria.

Drug-Target Affinity Davis (Davis et al., 2011) measures the binding affinities between kinase inhibitors and kinases, scored by the K_d value (kinase dissociation constant). KIBA (Tang et al., 2014) contains binding affinities for kinase inhibitors from different sources, including K_i, K_d and IC_{50}. KIBA scores (Öztürk et al., 2018) are constructed to optimize the consistency among these values.

Table 6: Summary for the molecule datasets for downstream tasks.

Dataset	Task	# Tasks	# Molecules	# Proteins	# Molecule-Protein
BBBP	Classification	1	2,039	–	–
Tox21	Classification	12	7,831	–	–
ToxCast	Classification	617	8,576	–	–
Sider	Classification	27	1,427	–	–
ClinTox	Classification	2	1,478	–	–
MUV	Classification	17	93,087	–	–
HIV	Classification	1	41,127	–	–
Bace	Classification	1	1,513	–	–
Delaney	Regression	1	1,128	–	–
Lipo	Regression	1	4,200	–	–
Malaria	Regression	1	9,999	–	–
CEP	Regression	1	29,978	–	–
Davis	Regression	1	68	379	30,056
KIBA	Regression	1	2,068	229	118,254

Input graph representation. For simplicity, we use a minimal set of node and bond features that unambiguously describe the two-dimensional structure of molecules following previous works (Hu et al., 2020). We use RDKit (Landrum et al., 2013) to obtain these features.

- Node features:
  - Atom number: $1 \sim 118$
  - Chirality tag: $\{\texttt{unspecified}, \texttt{tetrahedralcw}, \texttt{tetrahedralccw}, \texttt{other}\}$
- Edge features:
  - Bond type: $\{\texttt{single}, \texttt{double}, \texttt{triple}, \texttt{aromatic}\}$
  - Bond direction: $\{-, \texttt{endupright}, \texttt{enddownright}\}$

B MORE EXPERIMENTAL DETAILS

As we describe in the main text, we use the GIN architecture as the main encoder. To incorporate edge features, following previous works (Hu et al., 2020), we make some minor modifications to include bond features. Specifically, the raw node features and edge features are both 2-dimensional categorical vectors (see Appendix C for details), denoted as $(i_{v,1}, i_{v,2})$ and $(j_{e,1}, j_{e,2})$ for node v and edge e, respectively. Note that we also introduce unique categories to indicate masked nodes/edges as well as self-loop edges. As input features to GNNs, we first embed the categorical vectors by

$$\begin{aligned} h_v^{(0)} &= \mathrm{EmbNode}_1\left(i_{v,1}\right) + \mathrm{EmbNode}_2\left(i_{v,2}\right) \\ h_e^{(k)} &= \mathrm{EmbEdge}_1^{(k)}\left(j_{e,1}\right) + \mathrm{EmbEdge}_2^{(k)}\left(j_{e,2}\right) \text{ for } k = 0, 1, \ldots, K-1, \end{aligned}$$

where $\mathrm{EmbNode}_1(\cdot), \mathrm{EmbNode}_2(\cdot), \mathrm{EmbEdge}_1^{(k)}(\cdot)$, and $\mathrm{EmbNode}_1^{(k)}(\cdot)$ represent embedding operations that map integer indices to d-dimensional real vectors, and k represents the index of GNN layers. At the k-th layer, GNNs update node representations by

$$h_v^{(k)} = \mathrm{ReLU}\left(\mathrm{MLP}^{(k)}\left(\sum_{u \in \mathcal{N}(v) \cup \{v\}} h_u^{(k-1)} + \sum_{e=(v,u): u \in \mathcal{N}(v) \cup \{v\}} h_e^{(k-1)}\right)\right), \tag{11}$$

where $\mathcal{N}(v)$ is a set of nodes adjacent to v, and $e = (v, v)$ represents the self-loop edge. Note that for the final layer, i.e., $k = K$, we removed the ReLU from Eq. (11) so that $h_v^{(k)}$ can take negative values. This is crucial for pre-training methods based on the dot product, e.g., Context Prediction and Edge Prediction, as otherwise, the dot product between two vectors would be always positive.

The graph-level representation h_G is obtained by averaging the node embeddings at the final layer, i.e.,

$$h_G = \mathrm{Mean}\left(\left\{h_v^{(K)} \mid v \in G\right\}\right). \tag{12}$$

The label prediction is made by a linear model on top of h_G. In our experiments, we set the embedding dimension d to 300. For MLPs in Eq. (11), we use the ReLU activation with 600 hidden units. We apply batch normalization right before the ReLU in Eq. (11) and apply dropout to $h_v^{(k)}$ at all the layers except the input layer.

For tokenizer training, we adopt the above 5-layer GINs as the encoder and the decoder, which is trained for 60 epochs on the 2 million unlabeled molecules sampled from the ZINC15 database with batch size as 256 and the learning rate as 0.001. For TMCL, we set the masking ratios as 0.15 and 0.30, respectively. The temperature parameter τ is set to 0.1 and the margin m is set to 0.

C THE INFLUENCE OF THE MASKING RATIO

In this section, we study the influence of the masking ratio of MAM and Mole-BERT. As can be observed in Table 7, the performance increase when the masking ratio varies from 0.10 to 0.20 while witnessing a notable drop when the masking ratio varies from 0.20 to 0.30, which indicates over-large masking ratio will impair the GNNs pre-training. Additionally, as shown in Table 8, the masking ratio pairs of two branches in Mole-BERT matter for pre-training. Specifically, when the masking ratio pairs are with larger differences, the performance of Mole-BERT will be pronounced. Also, the performance of Mole-BERT drops sharply when the masking ratio pairs are both larger than 0.25.

Table 7: The performance with various masking ratios of MAM on 8 MoleculeNet datasets.

Masking ratio	0.10	0.15	0.20	0.25	0.30
MAM	71.64	72.16	72.12	71.51	71.36

Table 8: The performance with various masking ratio pairs of Mole-BERT on 8 MoleculeNet datasets.

Masking ratio pairs	(0.15, 0.20)	(0.15, 0.25)	(0.15, 0.30)	(0.20, 0.25)	(0.20, 0.30)	(0.25, 0.30)
Mole-BERT	73.02	73.81	74.04	72.95	73.72	72.33

D REGRESS THE FEATURES THAT ARE USED TO INFER THE ATOM LABELS.

In this section, we aim to investigate a possible alternative to MAM. Specifically, we try to regress the features that are used to infer the atom labels. Namely, the new pre-training objective is to regress the output of the group VQ-VAE (denoted as 'MAM (regress)'). As shown in Table 9, MAM or Mole-BERT with regressive pre-training objective consistently falls behind those with one-hot classification objective. This regressive objective may make the model over-fit to the noise or perturbations in the continuous values and hinders the models to learn high-level semantics.

Table 9: The performance on 8 MoleculeNet datasets.

Pre-training Tasks	MAM (regress)	MAM	Mole-BERT (regress)	Mole-BERT
Performance	71.37	72.16	73.43	74.04

E MORE RESULTS OF MOLECULE RETRIEVAL

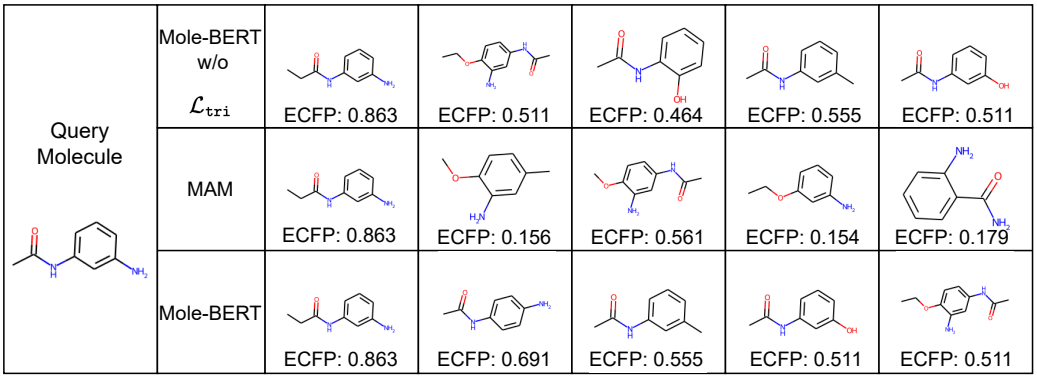

Figure 6: The query molecule and 5 closest molecules with the extracted representations.

We show more results of molecule retrieval in Figure 6, where 'Mole-BERT w/o $\mathcal{L}_{\texttt{tri}}$' means that we remove the triplet loss of Mole-BERT. As can be observed, the retrieval results of MAM are unsatisfactory. In contrast, both 'Mole-BERT w/o $\mathcal{L}_{\texttt{tri}}$' and 'Mole-BERT' can find chemically similar molecules in the database. However, 'Mole-BERT w/o $\mathcal{L}_{\texttt{tri}}$' fails to sort the molecules in a chemically meaningful order. Hence, the triplet loss is necessary and effective for Mole-BERT.

F TOKENIZATION FOR THE CHEMICAL BONDS

In addition to masking the atoms, Hu et al. (2020) also mask the chemical bond type and pre-train GNNs to predict them (4-way classification task). Similarly, this pre-training task is too simple for its small vocabulary ($\{\texttt{single}, \texttt{double}, \texttt{triple}, \texttt{aromatic}\}$). Additionally, the vocabulary is extremely unbalanced because the type of `single` bond is more common than other types. As a remedy, we mask the bond type and pre-train GNNs to predict the tokens of the two atoms that constitute the bond. Namely, we regard the pre-training task as a multi-label classification task, where two heads is adopted to predict the two tokens of the connected atom pairs, respectively. The results shown in Table 10 indicate that pre-training with both atoms and bonds attributes masking tasks is not superior to pre-training with only atom attributes masking. However, after we tokenize the chemical bonds, we achieve significant performance gains, which verifies that tokenization for the chemical bonds is necessary and effective.

Table 10: The performance of variants of MAM. 'Bonds AttMask' means that we mask the bond type and pre-train GNNs to predict them. 'MBM' means that we mask the bonds and pre-train GNNs to predict the connected atoms pairs' tokens.

Pre-training Tasks	MAM	MAM (+ Bonds AttrMask)	MAM (+ MBM)
Performance	72.16	72.08	72.63

G TIME COMPLEXITY OF MAM

Similar to AttrMask, the time complexity of MAM is linear with respect to the number of edges/nodes as it only involves sampling nodes/edges to be masked. Hence, it enjoys the same computational complexity as supervised training. The additional computational overhead originates from the memory consumption of the tokenizer. The pre-training of both MAM is nearly 24 hours, which is more time-consuming than AttrMask but the divergence is not significant.

H DISCRETE VAE V.S. GROUP VQ-VAE

Table 11: The comparisons between discrete vae and group VQ-VAE.

Pre-training Tasks	AttrMask	MAM (Discrete VAE)	MAM (Group VQ-VAE)
Performance	70.81	71.48	72.16

Both discrete VAE (Ramesh et al., 2021) and our group VQ-VAE can tokenize the atoms to compact codes. In Table 11, we compare their performance, from which we can observe that our group VQ-VAE outperforms discrete VAE by a significant margin. The reason is that group VQ-VAE can tokenize the atoms in a context-aware and semantics-aware manner. Also, group VQ-VAE can prevent the atoms of different types from being allocated with the same token id.

I TRAINING AND VALIDATION CURVES

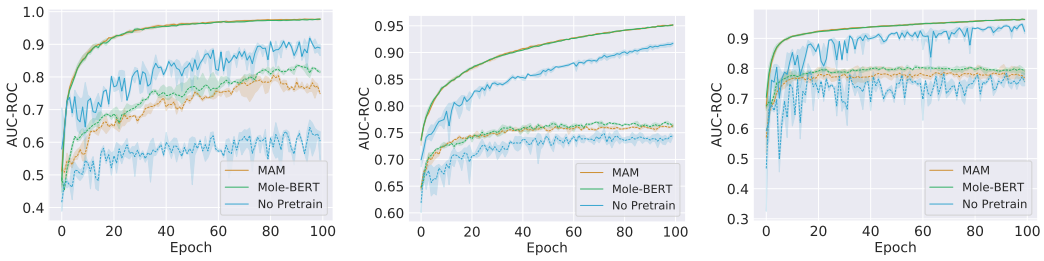

(a) ClinTox (b) Tox21 (c) Bace

Figure 7: Training (solid lines) and Validation (dashed lines) curves of various pre-training methods on ClinTox, Tox21, and Bace datasets.

We plot the training and validation curves in Figure 7, from which we can observe that the pre-trained models outperform training from scratch by significant margins. Additionally, for small-scale datasets such as Bace, training from scratch tends to overfit the training data of downstream tasks. In contrast, the pre-trained models can mitigate the over-fitting issue.

J GRAPHCL V.S. TMCL

GraphCL (You et al., 2020) is a representative contrastive pre-training strategy for molecular graphs. In this section, we compare GraphCL and TMCL as graph-level pre-training tasks. The results can

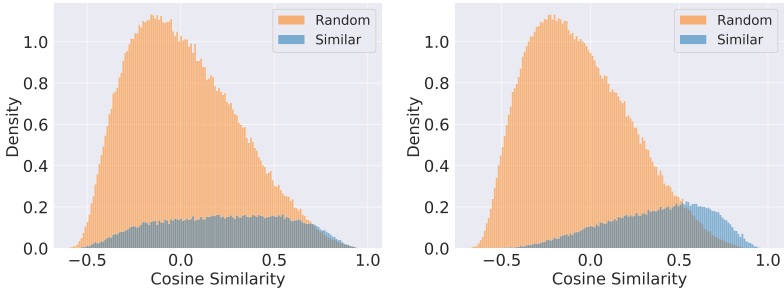

(a) MAM + GraphCL (b) MAM + TMCL (Mole-BERT)

Figure 8: Similarity histograms of MAM + GraphCL and Mole-BERT on Toxcast dataset.

be seen in Figure 8 and Table 12, from which we can observe that TMCL consistently outperforms GraphCL by considering the order of similarity between molecules.

Table 12: The comparisons between GraphCL and TMCL as graph-level pre-training tasks.

Pre-training Tasks	MAM	MAM + GraphCL	MAM + TMCL (Mole-BERT)
Performance	72.16	73.32	74.04

K DETAILED INFORMATION OF THE STRUCTURAL ABBREVIATIONS.

Table 13 shows the seven local structure categories of the carbons visualized in the main text.

Table 13: The first column lists the structural abbreviations corresponding to the legends. The second column list the corresponding chemical groups. The third column shows the structural formula.

Abbr	**Name**	**Structural Formula**
RPhF	Fluorophenyl	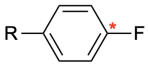
RCF_3	Trifluoromethyl	
RCHO	Aldehyde	
RCOOR’	Ester	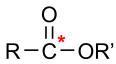
RCOR’	Ketone	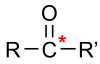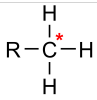
RCN	Nitrile	
RCH_3	Methyl